

Interpretation of the X-Ray Emission Spectra of Liquid Water through Temperature and Isotope Dependence

Osamu Takahashi¹, Ryosuke Yamamura², Takashi Tokushima³, and Yoshihisa Harada^{4,5}

¹*Basic Chemistry Program, Graduate School of Advanced Science and Engineering, Hiroshima University, Higashi-Hiroshima 739-8526, Japan*

²*Department of Chemistry, Hiroshima University, Higashi-Hiroshima 739-8526, Japan*

³*MAX IV Laboratory, Lund University, Fotongatan 2, 224 84 Lund, Sweden*

⁴*Institute for Solid State Physics (ISSP), University of Tokyo, Kashiwanoha, Kashiwa, Chiba 277-8581, Japan*

⁵*Synchrotron Radiation Research Organization, University of Tokyo, Sayo-cho, Sayo, Hyogo 679-5198, Japan*

 (Received 26 November 2021; accepted 31 January 2022; published 25 February 2022)

The interpretation of x-ray emission spectroscopy (XES) spectra in terms of their sensitivity to the hydrogen bonding and the consequent microheterogeneity in liquid water has been debated over a decade. To shed a light on this problem, we report the theoretical reproduction of the debated $1b_1$ peaks observed in the XES spectra of liquid water using semiclassical Kramers-Heisenberg formula. The essence of the temperature and isotope dependence of the $1b_1$ double peaks is explained by molecular dynamics simulations including full vibrational (O—H stretching, bending, and) modes, rotational combined with the density functional theory and core-hole induced dynamics. Some inconsistencies exist with the experimental XES profile, which illustrates the need to employ a more precise theoretical calculations for both geometry sampling and electronic structure using a more sophisticated procedure.

DOI: [10.1103/PhysRevLett.128.086002](https://doi.org/10.1103/PhysRevLett.128.086002)

Water is ubiquitous on earth and is one of the most important compounds in our lives. Despite its abundance, water exhibits many unusual physical properties [1]. Scientists have studied water using various techniques for over a century and proposed several interpretations of its structure. One of them is based on a two-structure model proposed by Röntgen [2], revisited by Wernet *et al.* [3], and followed by others [1,4,5]. Another is a uniform, continuous liquid model proposed by Bernal and Fowler [6] and followed by researchers in a wide range of fields [7–10]. X-ray spectroscopy is one of the various tools used to observe inhomogeneous features in both the solid and liquid phases. The interpretation of x-ray spectroscopy in terms of their sensitivity to the hydrogen-bond (H-bond) structure of liquid water has been debated, although comparable experimental data have been reported by different groups [11–13]. Several interpretations have been proposed for the double peak structures observed around 525–526 eV in x-ray emission spectroscopy (XES); these peak structures are designated as $1b_1$ -derived structures [14] by adopting the symmetry symbol of orbitals used for the gas phase of water. Tokushima *et al.* [11] reported that the double peaks possess the same symmetry and interpreted them as representing two different local H-bond structures, and Yamazoe *et al.* [13] updated it later. According to Fuchs *et al.* [12], the double peak structure can be reproduced by using a uniform, continuous liquid model and considering ultrafast O—H bond dissociation dynamics during the lifetime of the O $1s$ core hole.

Notably, both interpretations emphasize the importance of the H-bond feature in the liquid phase. The interpretation based on the two-structure model is now connected with the concept of low- and high-density amorphous liquids (LDL and HDL) at low temperatures [4]. Under ambient conditions, they correspond to different distributions of tetrahedrally coordinated water and water clusters with highly distorted or broken H bonds. Recently, Zhovtobriukh *et al.* [15] succeeded in theoretically reproducing the double $1b_1$ peaks in the XES spectra of liquid water by applying arbitrary sampling to molecular dynamics (MD) simulations.

Recent reports have discussed the dynamic effects on the resonantly excited state in liquid water using the resonant inelastic x-ray scattering technique [16,17]. Recently, Shi and Tanaka [18] reported the existence of two local structures in liquid water using x-ray scattering experiments and MD simulations. Cruzeiro *et al.* [19] theoretically analyzed the $1b_1$ peaks in the XES spectrum of liquid water, although core-hole-induced dynamics were absent in their simulations. They suggested that it is impossible to unambiguously attribute the split of the $1b_1$ peak to only two specific structural arrangements of the underlying H-bond network. Piskulich and Thompson [20] studied the temperature dependence of the oxygen-oxygen radial distribution function (RDF) of liquid water using MD simulations.

In the present Letter, we report the theoretical reproduction of the double $1b_1$ peak feature of XES in liquid

water. Several effects, such as geometry and dynamics, were discussed to determine the shape of the XES spectra.

To construct the structure of water in the liquid phase, classical MD simulations were adopted in the isothermal-isobaric ensemble from 270 to 360 K at intervals of 30 K and 1 bar using the GROMACS5.1.4 program package [21] with a TIP4Pew force field [22]. In a cubic simulation box, 1000 water molecules were included. The Verlet integrator was applied with a time step of 0.2 fs and run for 4 ns for each temperature point. The bond length and water molecule angles were fixed during the above simulations. However, they were relaxed to obtain power spectra, which were obtained by MD simulations in the microcanonical ensemble for 10 ps. To confirm the validity of our simulations, the oxygen-oxygen RDF between water molecules, density of water, and local structure index defined by Shiratani *et al.* [23,24] are included in Supplemental Material [25]. These results are consistent with those reported earlier [28–30].

The scheme of calculations of the XES spectra follows previous studies [31–33]. In brief, using the obtained final snapshot of the MD simulations, seventeen water clusters were extracted randomly. Two hundred clusters were sampled at 300 K, and one hundred clusters were sampled at temperature range used for sampling and for D₂O. We confirmed that the number of samplings was sufficient statistically to describe the XES spectra. XES spectra can be computed by the semiclassical Kramers-Heisenberg (SCKH) formula developed by Ljungberg *et al.* [34]. Two O–H bonds of the central water molecule in a sampled cluster were geometry optimized, and six positive vibrational frequencies of three rotations, H–O–H bending, and two O–H stretching modes were used in the analysis. To construct the total XES spectra, the contribution of the three translational modes can be neglected because the eigenvalues of these vibrational modes are lower than the thermal energy. Further, these effects are implicitly included by sampling other modes, consistent with the lower contribution of the translational mode in the power spectra analysis described later. At this step, it is necessary to construct a correct quantum mechanical distribution in the field of the surrounding water molecules. The multidimensional wave packet motions are modeled using classical MD simulations of the core-hole state with the initial conditions of quantum mechanical vibrational probability distribution along with a vibrational mode. Each trajectory runs 20 fs in steps of 0.25 fs. This MD simulation run is the minimum requirement to describe the effect of the dynamics on the core-hole state correctly. The spectra were calculated for each geometry along the MD trajectory. The final calculated spectra are shifted by -2.8 eV to match the experimental spectra. The lifetime of the O 1s core hole is considered as 4.1 fs [35]. The basis sets and functionals are the same as those used earlier for methanol [31] and ethanol [32]. To correct entanglement of the

potential energy curve and discontinuous of the transition moment, a new scheme with the genetic algorithm developed by Pettersson *et al.* [33] is applied. Density functional theory calculations were performed using the deMon2k program package [36].

Figure 1(a) shows the calculated XES spectra of liquid water from 270 to 360 K. The calculated spectra reproduced several experimentally observed features. We succeeded in reproducing the double peak features of the $1b_1$ state, which was observed in the experimental XES spectra [11–13]. And calculated XES spectra at low temperature is more resemblance to amorphous ice [11]. The calculated double $1b_1$ peaks are separated by approximately 0.8–1.5 eV depending on the temperature, which the experimental ones are reported as 0.7–0.9 eV [11] and 0.8 eV at the room temperature [13]. These values are slightly larger than the experimental values especially at the high temperature region, probably because of the procedure used for the initial geometries and the electronic structure calculations [37]. The relative intensity of the $1b_1$ state to the $1b_1$ and $3a_1$ states increased with temperature. Focusing on the $1b_1$ peak profiles, the lower side peak ($1b'_1$) was observed to be stable against increasing temperature, while the higher peak ($1b''_1$) shifted to a higher energy, as shown in Fig. 1(b). The $1b''_1$ peak intensity increased with increasing temperature. These features, which cannot be explained only by a simple two-state model, require other mechanisms such as density variation with temperature, which has already been discussed by Tokushima *et al.* [11]. Furthermore, the isotope dependence of the XES spectra of water at 300 K is shown in Fig. 1(c). The relative intensity of the $1b'_1$ peak to the $1b''_1$ peak is lower for D₂O, whereas it is higher for H₂O, suggesting that these differences call for a dynamical effect on the core-hole state. To extract the XES profile without core-hole induced dynamics, the XES spectra for the sampled initial structure of liquid water without time evolution are shown in Fig. 1(d). The electronic states examined are single valence hole states, corresponding to those probed by ultraviolet photoelectron spectroscopy (UPS). We theoretically obtained a single $1b_1$ peak whose energy position corresponds to the XES $1b''_1$ peak in Fig. 1(a) but with a narrower profile than the XES $1b''_1$ peak. The simulated spectra are consistent with the experimental UPS spectra obtained by Winter *et al.* [38], and the spectral profile was stable against temperature. Therefore, the specific structure observed by XES may be indistinguishable by UPS. The second peak, assigned as $1b'_1$, was reproduced by considering core-hole induced dynamics. However, the interpretation of the temperature dependence of XES is not straightforward.

To better understand the appearing features, our calculated spectra were classified into different types of H bonds. The H-bond criteria by Wernet *et al.* [3] were applied to examine the formation of H bonds. In the present study, the XES spectra were simply classified by the number of

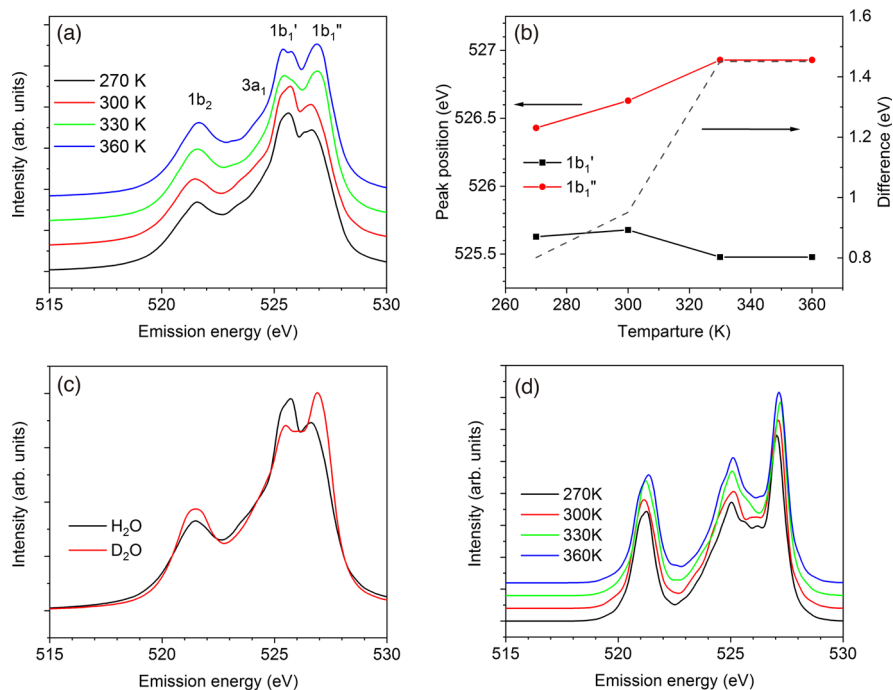


FIG. 1. (a) Temperature dependence of XES spectra of water from 270 to 360 K including the effect of core-hole induced dynamics. Inset of this figure set magnified around peak top of $1b_1$ states. (b) Peak position of $1b_1'$ and $1b_1''$ states (solid lines) and these energy difference (dashed line) from 270 to 360 K. (c) Isotope dependence of XES spectra of water at 300 K including the effect of core-hole induced dynamics. (d) Temperature dependence of XES spectra of water from 270 to 360 K without core-hole induced dynamics.

H bonds, i.e., H_m , where m is the sum of the number of H-bond donors and acceptors. Distinct spectra based on the number of H-bond donors and acceptors are included in Supplemental Material [25]. In the present study, we did not distinguish H-bond donors and acceptors to extract a simple picture related to the induced dynamics with a core hole. Figure 2(a) shows the XES spectra of water for several H-bond types at 300 K. The double peak features can be observed for all types of H bonds, but it is clear that the $1b_1'$ peak is more seen for the H4 and H3 structures. In the case of fewer H bonds, on the other hand, the intensity of the $1b_1''$ peak is higher than that of the $1b_1'$ peak. The $1b_1'$ peak is more related to tetrahedral structures but not being a simple peak but also a shoulder toward higher energy. Therefore, the $1b_1$ profile is determined by the contribution of both core-induced dynamics and H-bonded structures. Figure 2(b) shows the H-bond type distribution obtained by analyzing the geometries of the MD simulations. H4 and H2 correspond to a tetrahedrally coordinated cluster for a central water molecule and a distorted cluster, respectively. LDL and HDL include these local structures at different ratios. The main contribution is H3, which corresponds to the intermediate H-bond types between H2 and H4. For H1 and H2, the population increases monotonically with temperature. H3 and H4 display the opposite trend, while H5 has a minor contribution because the maximum coordination number of water by the H bond should be four. Our result is consistent with that of Miguel *et al.* [39]

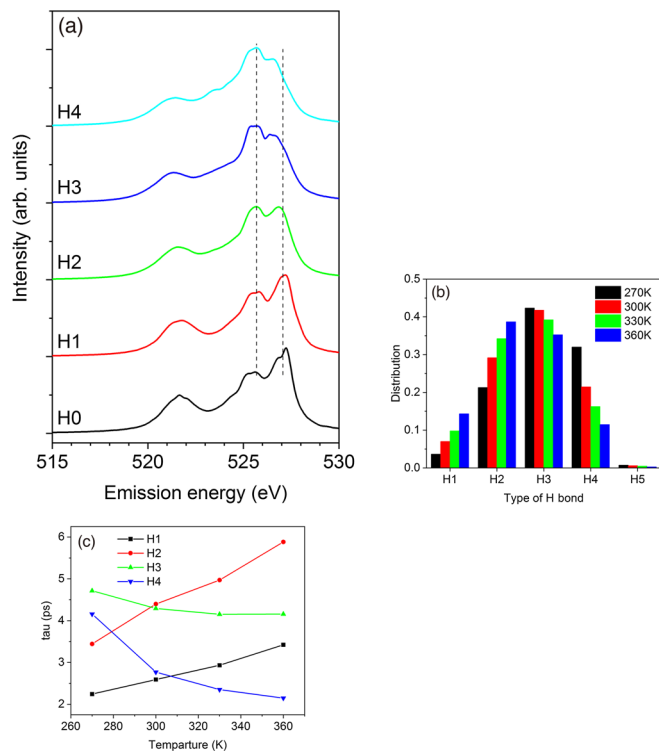


FIG. 2. (a) XES spectra of H_2O depending the type of H bonds at 300 K. H_n means that numbers of hydrogen bonds are n . (b) Distribution depending on the type of H bond from 270 to 360 K. (c) Lifetime of H bonds from 270 to 360 K depending of the number of H bonds using intermittent models.

in terms of the H-bond distribution. It should be noted that the H-bond distribution is directly reflected in the relative intensities of the $1b'_1$ and $1b''_1$ peaks in the XES spectra. And these discussions are also related to the XES spectra of amorphous ice [11]. Note that the closest oxygen-oxygen distance in ice Ih (hexagonal *ice* crystal) is 2.76 Å [40] and is shorter than that for liquid water of 2.8 Å [41]. Contrary to liquid water, most water molecules in amorphous ice may bind each other by a strong H bonding due to the short distance, which makes the dynamics faster than in the case of liquid water. Following the above discussion, the intensity of $1b'_1$ peak in amorphous ice would be enhanced than that of $1b''_1$ peak. The same MD simulation also enabled us to estimate the H-bond lifetime following the method of Rapaport [42]. The H-bond lifetime was evaluated using the relaxation time constant τ , estimated from the exponential decay of the autocorrelation function, in the form of

$$C(t) = \frac{\sum_{ij} s_{ij}(t_0)s_{ij}(t_0 + t)}{\sum_{ij} s_{ij}(t_0)}, \quad (1)$$

where $s_{ij}(t)$ is unity if molecules i and j are bonded at time t and zero if there is no bond. The results of applying the intermittent model in the present study are shown in Fig. 2(c). The values obtained were comparable to those reported by Antipova *et al.* [43]. The lifetimes of H1 and H2 increased with increasing temperature, whereas H3 and H4 exhibited the opposite trend. At low temperatures, highly coordinated configurations, such as H4, were dominant and possessed a longer lifetime. In contrast, H2 was important at high temperatures. The relative intensities of the $1b'_1$ and $1b''_1$ peaks in the XES spectra [Fig. 2(a)] reflect this situation. The time propagation of XES was examined to analyze the effect of the core-hole induced dynamics on the spectra. Figure 3(a) shows the 20 fs propagation of the XES spectra for H4 at 300 K. The

time propagations for other types of H bonds are available in Supplemental Material [25]. The main features are similar, suggesting that the effect of the core-hole induced dynamics is similar among all the types of H bonds. We focused on the peak shift and intensity modulation of the $1b_1$ peak, which is stable for the first few femtoseconds after core excitation. It then starts to move toward lower energy, gradually decreasing in intensity. The rate of the highest peak position and intensity over time, as a function of the number of H bonds, are plotted in Fig. 3(b). Except for the intensity decay of H1, increasing the number of H bonds decreases both the rates, indicating that the increase in the number of H bonds accelerates the core-hole induced dynamics, probably owing to the electrostatic field of the surrounding molecules. As shown in Figs. 1(c) and 1(d), the isotope effect and the absence of temperature effect without core-hole induced dynamics show the influence of core-hole induced hydrogen atom dynamics on the XES spectra. The peak shift of the $1b_1$ state is suppressed by increasing the mass from hydrogen to deuterium, causing an increase in the $1b''_1$ peak, as observed in previous studies [11,12].

Next, we examined the effect of thermally excited vibrational modes on the XES spectra. In a previous study, Zhovtobriukh *et al.* included thermal effects to simulate the XES spectra of liquid water by incorporating two O—H stretch modes [15]. These two vibrational modes should be sufficient for describing the effect of H-bond dynamics because they have a much deeper potential energy surface than the other modes. In the present Letter, we considered the effects of the other modes on the XES spectra. For a water molecule in a liquid, more than three internal modes can be obtained: antisymmetric and symmetric O—H stretching, bending, three rotational, and three translational modes. The latter six modes were assigned as intermolecular modes. By optimizing the geometry of the central water molecule, we obtained nine independent vibrational modes and examined their effects on the XES spectra using the SCKH scheme [34]. The results at 300 K are summarized in Fig. 4. As discussed above, the effects of core-hole induced dynamics are similar. Instead, the difference is whether excited vibrational modes are along the H-bond direction. Since motion along the direction of the H bonds is expected to accelerate the peak shift, the deviation from the O—H bond direction, including the core-excited oxygen atom, should influence the spectra more effectively. When the O—H stretching modes are excited, core-hole induced hydrogen atom dynamics along the O—H bond line are accelerated, which increases the $1b'_1$ peak. However, exciting the vibrational modes that move the hydrogen atom perpendicular to the line of the O—H bond suppresses the core-hole induced dynamics, decreasing the $1b'_1$ peak. This mode sensitivity to the XES $1b_1$ profile may depend on the depth of the potential energy surface of the O—H stretching mode.

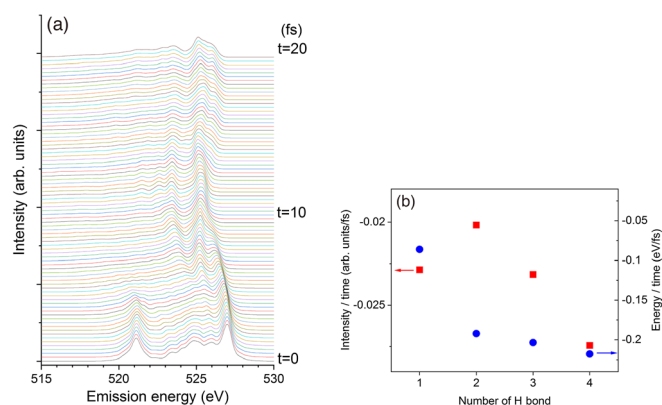


FIG. 3. (a) Time propagation of XES spectra at 300 K for the case of four H bonds during 20 fs. (b) Rate of highest peak position (blue circle) and the intensity (red square) over time as a function of the number of H bonds.

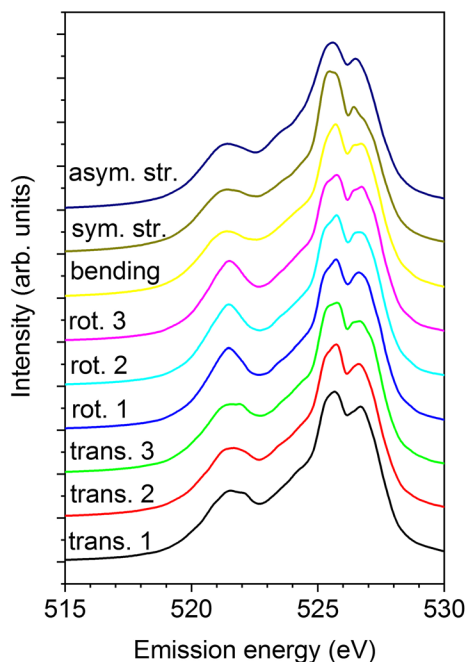


FIG. 4. XES spectra for each vibrational mode at 300 K. The spectra is stacked as increasing the vibrational number. “asym. str.” and “sym. str.” mean antisymmetric and symmetric stretching modes.

The key parameters determining the XES $1b_1$ profile are the density of water and the orientation of water molecules surrounding the core-excited water molecule as a function of the temperature. In liquid water, the decrease in the density of water, arising from an increase in its temperature from 4°C at maximum density, may produce less effective core-hole induced dynamics, as discussed in Fig. 3(b), and contributes to the increase of the $1b_1''$ peak at higher temperatures. However, when the temperature is decreased from 4°C, the influence of the density of water is dominated by other effect, namely, the alignment of hydrogen bonds along the O—H bond axis direction, as evident from the increase in the four-coordinate H bonds, shown in Fig. 2(b). This effect accelerates the core-hole induced dynamics, and the $1b_1'$ peak should dominate. Therefore, the relative intensity between the $1b_1'$ and $1b_1''$ peaks may be sensitive to various physical properties, such as the local density around the excited water molecule, number of H bonds, and the H-bond orientational distribution.

We successfully reproduced the XES spectra of liquid water by incorporating the effect of full vibrational modes, O—H stretching, bending, and rotational modes of liquid water. Both temperature and isotope dependence were explained by considering the H-bond configuration around the excited water molecule and core-hole induced dynamics. The present procedure is generalized and may be applied to future studies on aqueous conditions. Several issues remain, especially the reproducibility of the splitting

energy of the $1b_1'$ and $1b_1''$ peaks, which is consistent with the experiment at room temperature, but not at high temperature. These may be refined further by precise theoretical calculations for both geometry sampling and electronic structure using a more sophisticated procedure. It should be noted that our analyses are consistent with those conducted by Tokushima *et al.* [11] and Fuchs *et al.* [12]. We hope that our research resolves the debates on the interpretation of the structure of liquid water.

The authors thank Professors Lars Pettersson and Anders Nilsson at Stockholm University for fruitful comments and stimulating discussions. We would like to thank the Research Center for Computational Science, Okazaki, and the Research Institute for Information Technology at Kyushu University, Fukuoka, Japan. This work was supported by JSPS KAKENHI Grant No. JP19H05717 (Grant-in-Aid for Scientific Research on Innovative Area: Aquatic Functional Materials).

- [1] P. Gallo *et al.*, *Chem. Rev.* **116**, 7463 (2016).
- [2] W. C. Röntgen, *Ann. Phys. (Berlin)* **281**, 91 (1892).
- [3] P. Wernet *et al.*, *Science* **304**, 995 (2004).
- [4] A. Nilsson and L. G. M. Pettersson, *Nat. Commun.* **6**, 8998 (2015).
- [5] P. H. Handle, T. Loerting, and F. Sciortino, *Proc. Natl. Acad. Sci. U.S.A.* **114**, 13336 (2017).
- [6] J. D. Bernal and R. H. Fowler, *J. Chem. Phys.* **1**, 515 (1933).
- [7] W. L. Jorgensen, J. Chandrasekhar, J. D. Madura, R. W. Impey, and M. L. Klein, *J. Chem. Phys.* **79**, 926 (1983).
- [8] R. A. Marcus, *J. Chem. Phys.* **24**, 966 (1956).
- [9] G. C. Pimentel and A. L. McClellan, *The Hydrogen Bond* (Freeman, San Francisco, 1960).
- [10] G. N. I. Clark, C. D. Cappa, J. D. Smith, R. J. Saykally, and T. Head-Gordon, *Mol. Phys.* **108**, 1415 (2010).
- [11] T. Tokushima, Y. Harada, O. Takahashi, Y. Senba, H. Ohashi, L. G. M. Pettersson, A. Nilsson, and S. Shin, *Chem. Phys. Lett.* **460**, 387 (2008).
- [12] O. Fuchs *et al.*, *Phys. Rev. Lett.* **100**, 027801 (2008).
- [13] K. Yamazoe, J. Miyawaki, H. Niwa, A. Nilsson, and Y. Harada, *J. Chem. Phys.* **150**, 204201 (2019).
- [14] T. Tokushima, Y. Horikawa, H. Arai, Y. Harada, O. Takahashi, L. G. M. Pettersson, and A. Nilsson, *J. Chem. Phys.* **136**, 044517 (2012).
- [15] I. Zhovtobriukh, N. A. Besley, T. Fransson, A. Nilsson, and L. G. M. Pettersson, *J. Chem. Phys.* **148**, 144507 (2018).
- [16] V. Vaz da Cruz *et al.*, *Nat. Commun.* **10**, 1013 (2019).
- [17] V. Vaz da Cruz *et al.*, *J. Chem. Phys.* **150**, 234301 (2019).
- [18] R. Shi and H. Tanaka, *J. Am. Chem. Soc.* **142**, 2868 (2020).
- [19] V. W. D. Cruzeiro, A. Wildman, X. Li, and F. Paesani, *J. Phys. Chem. Lett.* **12**, 3996 (2021).
- [20] Z. A. Piskulich and W. H. Thompson, *J. Chem. Phys.* **152**, 011102 (2020).
- [21] M. J. Abraham, T. Murtola, R. Schulz, S. Páll, J. C. Smith, B. Hess, and E. Lindahl, *SoftwareX* **1–2**, 19 (2015).

- [22] H. W. Horn, W. C. Swope, J. W. Pitera, J. D. Madura, T. J. Dick, G. L. Hura, and T. Head-Gordon, *J. Chem. Phys.* **120**, 9665 (2004).
- [23] E. Shiratani and M. Sasai, *J. Chem. Phys.* **104**, 7671 (1996).
- [24] E. Shiratani and M. Sasai, *J. Chem. Phys.* **108**, 3264 (1998).
- [25] See Supplemental Material at <http://link.aps.org/supplemental/10.1103/PhysRevLett.128.086002> for lifetime dependence of XES spectra of water, power spectra of H₂O by velocity autocorrelation functions, and XES spectra with different sampling scheme, which includes Refs. [26,27].
- [26] M. Neeb, J.-E. Rubensson, M. Biermann, and W. Eberhardt, *J. Electron Spectrosc. Relat. Phenom.* **67**, 261 (1994).
- [27] T. Yagasaki and S. Saito, *Annu. Rev. Phys. Chem.* **64**, 55 (2013).
- [28] D. Schlesinger, K. T. Wikfeldt, L. B. Skinner, C. J. Benmore, A. Nilsson, and L. G. M. Pettersson, *J. Chem. Phys.* **145**, 084503 (2016).
- [29] J. L. F. Abascal and C. Vega, *J. Chem. Phys.* **123**, 234505 (2005).
- [30] K. T. Wikfeldt, A. Nilsson, and L. G. M. Pettersson, *Phys. Chem. Chem. Phys.* **13**, 19918 (2011).
- [31] M. P. Ljungberg, I. Zhovtobriukh, O. Takahashi, and L. G. M. Pettersson, *J. Chem. Phys.* **146**, 134506 (2017).
- [32] O. Takahashi, M. P. Ljungberg, and L. G. M. Pettersson, *J. Phys. Chem. B* **121**, 11163 (2017).
- [33] L. G. M. Pettersson and O. Takahashi, *Theor. Chem. Acc.* **140**, 162 (2021).
- [34] M. P. Ljungberg, A. Nilsson, and L. G. M. Pettersson, *Phys. Rev. B* **82**, 245115 (2010).
- [35] R. Sankari, M. Ehara, H. Nakatsuji, Y. Senba, K. Hosokawa, H. Yoshida, A. De Fanis, Y. Tamenori, S. Aksela, and K. Ueda, *Chem. Phys. Lett.* **380**, 647 (2003).
- [36] A. M. Köster *et al.*, *deMon2k*, (The deMon developers, 2018).
- [37] O. Takahashi and L. G. M. Pettersson, *J. Chem. Phys.* **121**, 10339 (2004).
- [38] B. Winter, R. Weber, W. Widdra, M. Dittmar, M. Faubel, and I. V. Hertel, *J. Phys. Chem. A* **108**, 2625 (2004).
- [39] B. Miguel, J. Zúñiga, A. Requena, and A. Bastida, *J. Phys. Chem. B* **118**, 9427 (2014).
- [40] A. Goto, T. Hondoh, and S. Mae, *J. Chem. Phys.* **93**, 1412 (1990).
- [41] A. H. Narten and H. A. Levy, *J. Chem. Phys.* **55**, 2263 (1971).
- [42] D. C. Rapaport, *Mol. Phys.* **50**, 1151 (1983).
- [43] M. L. Antipova and V. E. Petrenko, *Russ. J. Phys. Chem.* **87**, 1170 (2013).